

Automatic Synthesis of Neurons for Recurrent Neural Nets

Roland Olsson

Chau Tran

Lars Magnusson

Department of Computer Science

Østfold University College

N-1757 Halden, Norway

ROLAND.OLSSON@HIOF.NO

CHAU.TRAN@HIOF.NO

LARS.MAGNUSSON@HIOF.NO

Abstract

We present a new class of neurons, ARNs, which give a cross entropy on test data that is up to three times lower than the one achieved by carefully optimized LSTM neurons. The explanations for the huge improvements that often are achieved are elaborate skip connections through time, up to four internal memory states per neuron and a number of novel activation functions including small quadratic forms.

The new neurons were generated using automatic programming and are formulated as pure functional programs that easily can be transformed.

We present experimental results for eight datasets and found excellent improvements for seven of them, but LSTM remained the best for one dataset. The results are so promising that automatic programming to generate new neurons should become part of the standard operating procedure for any machine learning practitioner who works on time series data such as sensor signals.

Keywords: Recurrent neural nets, neuron synthesis, automatic programming

1. Introduction

Time series or sequence data is abundant in machine learning and range from signal processing to stock prices and more complex data such as natural language. Indeed, the entire life of a human being is also a time series dataset generated by the five senses.

This paper focuses on improving LSTM neurons (Hochreiter and Schmidhuber, 1997) since they both are theoretically interesting and also one of the most popular and effective machine learning tools.

By using the ADATE automatic programming system (Olsson, 1995), we generated new neurons for each specific dataset and found that they were up to three times better than LSTM as measured by cross entropy on test data. We used eight datasets with between 22 and 500 timesteps and found the biggest improvement for the 500 timestep dataset.

The main novelties of the ADATE Recursive Neurons (ARNs) are as follows.

1. ARNs often contain skip connections like in Highway nets and ResNet, but through the time dimension.
2. Up to four memory states per neuron instead of just one as in the LSTM.
3. Novel activation functions built from, for example, small quadratic forms and sequences of a set of three predefined and well known activation functions.

4. A given neuron may use linear combinations of the states of other neurons.
5. Differentiating between recurrent output as well as state values from “self” and “all others”.

We will now give an overview of the paper. First, we present related work on automatic programming and evolution of recurrent neurons. The next section describes how to represent ARNs in a small and purely functional subset of the Standard Meta Language (SML) (Milner et al., 1997) and also gives a compact and purely functional definition of the classic LSTM as an illustration. We then provide experimental results for eight medium size datasets that typically are found in practical sensor data analysis applications. We finish by some conclusions and a glimpse of the almost infinite possibilities for future work that are enabled by the technology in this paper. The appendix contains seven examples of ARNs to exhibit some of their novelties.

2. Related work

Long short-term memory (LSTM) was originally presented in Sepp Hochreiter’s masters thesis (Hochreiter and Schmidhuber, 1997) with Jürgen Schmidhuber as the advisor and made more well known by Hochreiter and Schmidhuber (Hochreiter and Schmidhuber, 1997).

It remains a quite popular and competitive technology also 25 years later, which is remarkable in a rapidly developing field such as machine learning. We assume that the reader already is familiar with LSTMs and will not describe them here.

Some newer and prominent recurrent neurons that sometimes outperform LSTM include Gated Recurrent Units (Cho et al., 2014) and Independently Recurrent Neural Nets (Li et al., 2018).

2.1 Using evolutionary computation to synthesize recurrent neurons

Galvan and Mooney (Galván and Mooney, 2021) provide an extensive review of neuroevolution and show that the field primarily deals with using evolutionary methods for hyperparameter or architecture and topology search for entire neural nets using a predefined set of neuron types. They do not mention any work that evolves the neurons themselves.

An early attempt to evolve neurons using ADANTE was made by Berg et. al. (Berg et al., 2008), but these neurons were a special type of spiking neurons for segmentation of gray scale images containing noisy rectangles. Although reasonable improvements were found, the results are not practically competitive and have been superseded by modern CNN based nets for image processing.

A key distinction between different approaches to neuron evolution is whether the goal is to find a general neuron that is better for a large class of datasets or whether it is to produce more specialized neurons that work best for an application specific class of datasets. Our goal is to produce superior and application specific neurons whereas Bayer et. al (Bayer et al., 2009) and Jozefowicz et. al. (Jozefowicz et al., 2015) try to produce more general replacements for the LSTM, which may be much more difficult to achieve.

Of course, the disadvantage with application specific neurons, for example neurons specialized for high frequency trading, is that it is more difficult to replace the neuron itself

in the well known neural toolboxes than it is to just optimize the hyperparameters and the architecture. A possible advantage though is that much bigger application specific improvements may be found. Thus, we argue that all three of overall architecture, hyperparameters and neuron design need to be optimized for the best results.

Bayer et. al (Bayer et al., 2009) mention another distinction, namely if a very indirect representation such as DNA is employed to represent neurons or whether transformations such as so-called “mutations” are performed directly on the neuron circuits. They use the latter approach and define a number of well designed transformations on a directed acyclic graph representation of neurons. Thus, they build an evolutionary system from scratch expressly for evolving LSTM replacements. Our approach is a bit different since we use the universal ADATE automatic programming system and do not code any evolutionary search nor any transformations specifically for neuron evolution.

Jozefowicz et. al. (Jozefowicz et al., 2015) also build their evolutionary computation system from scratch and excel in neural architecture design and hyperparameter search. It is obvious from the paper that they have deep expertise in these areas. In contrast to us, they perform hyperparameter search on-the-fly during the evolution. As a result of this and other experimental choices, they evaluate a number of new neuron candidates that is about five orders of magnitude smaller than we did with ADATE.

2.2 Automatic design of algorithms through evolution

Automatic design of algorithms through evolution (ADATE) (Olsson, 1995) was originally developed for automatic synthesis of symbolic and recursive functional programs, but a few years later also given simple mechanisms for optimizing floating point constants. It writes programs in a very small subset of SML (Milner et al., 1997), which was conceived by Robin Milner as a meta language for symbolic logic (Gordon et al., 1978). As we will see in this paper, it is also quite suitable for meta machine learning.

Some other and fundamentally different approaches to inductive programming, that are more suitable for explainable machine learning than ADATE, are discussed in the JMLR special issue edited by (Kitzelmann et al., 2006).

ADATE has the ability to invent help functions as they are needed and to perform so-called lifting and distribution transformations on case- and let-expressions as well as many other semantics preserving and useful program transformations (Olsson, 1995). However, the details of these are beyond the scope of the current paper.

ADATE needs a specification of the problem to be solved. A specification contains the following primary ingredients.

1. Algebraic datatypes, for examples various lists and trees.
2. A signature for the function f that is to be synthesized and optionally also an initial definition of that function.
3. An evaluation function that tests a synthesized function on a number of training inputs. Note that f may occur as a small part of a big program and that calculating f typically means to run this program on the training inputs. Thus, ADATE performs symbolic reinforcement (meta-)learning.

Given the specification, ADATE runs on a cluster where many programs are transformed and evaluated in parallel. The result is a Pareto front of gradually more syntactically complex and better programs. Syntactic complexity is the sum of the base-2 logarithm of the occurrence probabilities of the symbols in all nodes in the syntax tree of a program. It falls on the human operator of ADATE to select a suitable program from the Pareto front. Below, we will make it simple and always choose the one that has the lowest mean squared error or cross entropy on validation data.

3. How to represent ARNs as functional programs

We will first explain how to represent neurons and then explain how a neuron is a transition function from one timestep to the next. Then, we will give a functional program corresponding to an LSTM neuron as an example.

3.1 Datatypes

A key ingredient in neural nets is linear combination of a set of floating point values and we will start by explaining how to represent this using algebraic datatypes. For example, consider a linear combination of two values x_1 and x_2 using weights w_1 and w_2 and bias b .

$$w_1x_1 + w_2x_2 + b$$

In our algebraic datatype, we abstract away the weights and represent a linear combination using the SML type `linComb`, defined below, with two constructors `bias` and `cons`. The `*` is Cartesian product and the `|` introduces a sum type.

```
datatype linComb = bias | cons of real * linComb
```

This is essentially the type of lists that always contain at least one value, namely a bias. The type `real` represents floating point numbers in spite of its SML name. The linear combination above would correspond to the following list.

```
cons( x1, cons( x2, bias ) )
```

At this point, the reader perhaps wonder how on earth the weights will be specified. The answer is that we only allow a limited number of weight mappings, where each mapping is indicated by a function called `lc i` for $i = 0, 1, \dots, n$ for $n + 1$ mappings. The current implementation has $n = 4$, which means that there will be five different sets of forward, recurrent and peep weight matrices.

The expression below will be translated by our compiler to the linear combination above assuming that mapping 0 has weights w_1 and w_2 and bias b .

```
lc0( cons( x1, cons( x2, bias ) ) )
```

However, if we were to use say `lc1` instead of `lc0`, another bias and set of weights would be used after compilation.

3.2 Transition function

It is now time to start explaining how to represent recursive neural net neurons and their internal and external connections.

To introduce our notation, let us first consider the transition function f of type $\mathbb{R}^2 \rightarrow \mathbb{R}$ for a simple RNN neuron with input $x^{(t)}$ and output $y^{(t)}$ at time t . Thus, the inputs and outputs of f are as follows.

$$f(x^{(t)}, y^{(t)}) = y^{(t+1)}$$

An LSTM neuron has an internal state s which means that its type is $\mathbb{R}^3 \rightarrow \mathbb{R}^2$.

$$f(x^{(t)}, s^{(t)}, y^{(t)}) = (s^{(t+1)}, y^{(t+1)})$$

An ADATE recursive neuron (ARN) has four internal states instead of just one which implies that it could be a function with the following signature.

$$f(x^{(t)}, s_0^{(t)}, s_1^{(t)}, s_2^{(t)}, s_3^{(t)}, y^{(t)}) = (s_0^{(t+1)}, s_1^{(t+1)}, s_2^{(t+1)}, s_3^{(t+1)}, y^{(t+1)})$$

However, we will differentiate between the output from the neuron itself at timestep t and the linear combination of the outputs of the other neurons in the same layer. This “recognition of self” turns out to be an important feature of ARNs as shown by the experimental results in Section 4.4.

Experimentally, we also found that skip connections through time were invented by ADATE and it is easy to see that this is enabled by having many internal states instead of just one. For example, if we wish the output at timestep t to be available as an input at timestep $t + 2$, we can choose $s_1^{(t+1)}$ to $y^{(t)}$ and $s_2^{(t+1)}$ to $s_1^{(t)}$. Many other and much more intricate ways of curating information through time are possible and have been invented by ADATE.

3.3 Functional programming definition of an ARN

In order to explain the signature of an ARN, we will switch to functional programming notation and start by explaining the input parameters.

InputsLC : `linComb`. The list of inputs.

SelfPeep0 : `real`. State $s_0^{(t)}$.

SelfPeep1 : `real`. State $s_1^{(t)}$.

SelfPeep2 : `real`. State $s_2^{(t)}$.

SelfPeep3 : `real`. State $s_3^{(t)}$.

SelfOutput : `real`. The current output value y_t .

OtherPeepsLC : `linComb`. The list of the $s_0^{(t)}$ values of all other nodes in the layer.

OtherOutputsLC : **linComb**. The list of the $y^{(t)}$ values of all other nodes in the layer.

Finally, we will explain how variables are bound to values of expressions in the small subset of SML used in ADATE. The syntax is a bit unusual and relies on case-expressions for this. For example, the case-expression below means that the variable **V** will represent the value of the expression **E1** and that its scope is **E2**.

```
case E1 of V => E2
```

Of course, these case expressions are used to construct functional programs that correspond to directed acyclic graphs (DAGs) in neural circuit diagrams.

Consider the usual LSTM neuron with peepholes in Figure 1 that is a direct translation of the LSTM circuit diagram in (Greff et al., 2016). We now have everything that is needed to understand the functional programming definition of this neuron. Figure 1 contains five case-expressions before giving the output tuple in which only the first and the last fields are used and the three in the middle just contain dummy values, in this case 0.0, since they are not needed for LSTM. Recall that the output quintuple first contains the four next states and then the next output as its last field. Since all our datasets are centered and scaled, it turns out that biases are almost totally redundant in the LSTM, which means that they have been omitted in Figure 1.

As another example, we will explain a rather simple neuron synthesized by ADATE and that comes from the Pareto front for Double pendulum discussed later in Section 4.6.

The program corresponding to the neuron is given in Figure 2. The auxiliary function **g** has been invented by ADATE. Its purpose is to bind **S0** to the **tanh** expression. The return value of **g** is a quintuple where the last field is a quadratic polynomial that gives the output from the neuron. The first field is just **S0**, which will become **SelfPeep0** for the next timestep. A linear combination of these values for the other neurons than “self” will become **OtherPeepsLC**.

Figure 3 shows a more traditional representation of the neuron with one copy of the neuron for timestep t and another for $t + 1$ with dashed lines indicating information flow across timesteps. The figure uses linear algebra notation with bold lower case variables being vectors, whereas bold upper case variables represent matrices. The vector of state 0 values is \mathbf{s}_0 , corresponding to the scalar variable **S0** in the program above. The input weight matrices \mathbf{U}_1 and \mathbf{U}_2 correspond to the weight mappings indicated by **lc1** and **lc2** respectively. The recurrent weight matrix \mathbf{W}_0 is hollow, that is has zeroes along its diagonal to exclude “self” from **OtherPeepsLC**. The vector \mathbf{a}_0 contains so-called auxiliary weights and is multiplied element-wise (Hadamard product) as indicated by the operator \odot . It is not really needed here but corresponds to how the **cons** is translated by our compiler.

The shaded boxes in the diagram implicitly contain weight vectors and matrices, which have been omitted in order not to clutter the diagram.

The intermediate vector $\mathbf{s}_{0,0}$ represents **lc2 InputsLC + SelfPeep0** and $\mathbf{s}_{0,1}$ represents **lc1(cons(lc0 OtherPeepsLC, InputsLC))**. When we introduce new intermediate variables, we use a second subscript as above to differentiate them

In our actual C++ code, all input weight matrices are stacked in one matrix and the same goes for all recurrent weight matrices in order to reduce the number of matrix-vector multiplications.

```

case
  tanh(
    lc0 InputsLC + lc0( cons( SelfOutput, OtherOutputsLC ) )
  )
of Z =>
case
  sigmoid(
    lc1 InputsLC +
    lc1( cons( SelfPeep0, cons( SelfOutput, OtherOutputsLC ) ) )
  )
of I =>
case
  sigmoid(
    1.0 + lc2 InputsLC +
    lc2( cons( SelfPeep0, cons( SelfOutput, OtherOutputsLC ) ) )
  )
of F =>
case F * SelfPeep0 + I * Z of S0 =>
case
  sigmoid(
    lc3 InputsLC +
    lc3( cons( S0, cons( SelfOutput, OtherOutputsLC ) ) )
  )
of 0 =>
  ( S0, 0.0, 0.0, 0.0, 0 * tanh S0 )

```

Figure 1: The LSTM neuron with peepholes as a functional program.

```

let
  fun g S0 = ( S0, S0, S0, S0, S0 - S0 * S0 )
in
  g(
    tanh(
      relu( lc2 InputsLC + SelfPeep0 ) -
      lc1( cons( lc0 OtherPeepsLC, InputsLC ) )
    )
  )
end

```

Figure 2: A small neuron for modeling a double pendulum.

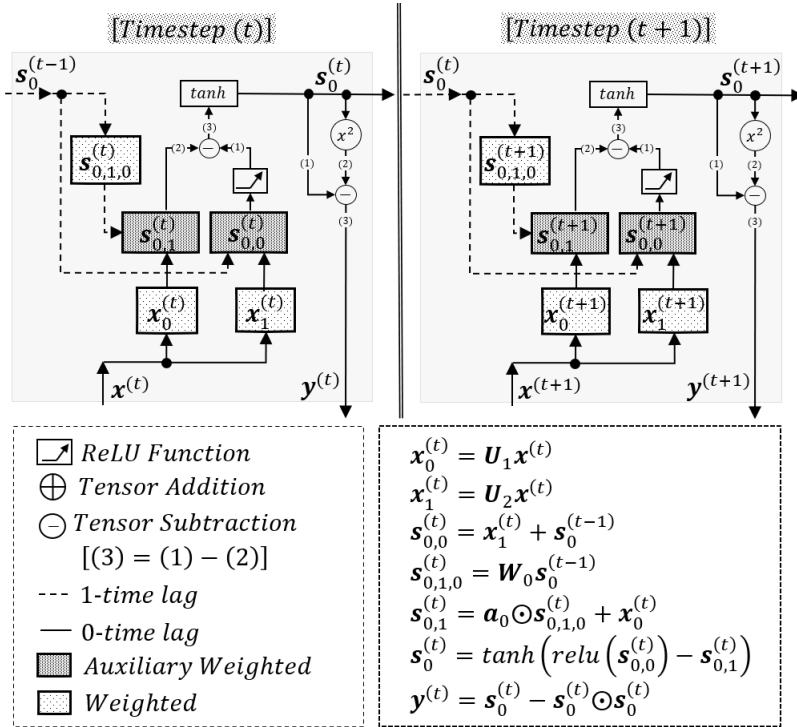


Figure 3: A circuit diagram for the neuron in Figure 2.

3.4 Choosing activation functions

ADATE needs to be given a set of predefined functions to use for program synthesis. Obviously, we include addition, subtraction, multiplication and division. It would be possible for ADATE to use these together with if-expressions to synthesize its own activation functions, for example ReLU (Fukushima, 1969) or good approximations of the hyperbolic ones, but after some preliminary experimentation we decided against using if-expressions altogether.

Instead, we chose to include three predefined activation functions, which turn out to be very useful for synthesizing other and novel activation functions.

First, we chose to include `tanh` but not sigmoid since ADATE easily can express it as a scaled version of `tanh`.

Second, the `relu` function was included and after that we also chose to add a linear approximation of `tanh` which we called saturated ReLU (`srelu`). The latter is defined as being the identity function for values between -1 and 1, just 1 for values greater than 1 and -1 for values less than -1. It could be implemented using two ReLU functions, but we chose to relieve ADATE of that extra burden.

Our intuition was that elimination of the more curved parts of `tanh` may lead to smaller problems with vanishing gradients since `relu` also is linear and seems to have this advantage. However, we still wanted a function more suitable for gating than `relu` and therefore defined `srelu`.

Thus, our set of predefined activation functions is `tanh`, `relu` and `srelu`.

4. Experiments

In this section, we will first explain our neural net architecture and hyperparameter optimization, then how to very quickly evaluate neuron candidates and then introduce the datasets that we tested ARN on. Finally, we will present the experimental results along with statistical analyses.

In general, we always split datasets into three subsets, with 50% for training, 25% for validation and 25% for testing. The test set is used only once at the very end to prevent subtle forms of information leaks and the overfitting that may result.

4.1 Architecture and hyperparameter optimization

Before starting an ADATE run for a new dataset, we optimized the architecture and the hyperparameters for LSTM and used these also for the neurons discovered by ADATE. Assume that we have a dataset with n_o outputs and that there are l nodes in the LSTM layer.

We used the simple net architecture below.

1. An LSTM layer with l nodes.
2. A hyperbolic tangent layer with n_o nodes.
3. A linear layer with n_o nodes.

We use Glorot initialization for forward weights and orthogonal initialization for recurrent weights with a scaling factor of 0.1 in both cases. Also, we use an initial extra bias of 1 for the forget gates as recommended by (Jozefowicz et al., 2015) and others.

The loss function was mean squared error (MSE) for regression and softmax plus cross entropy for classification. We tried a variety of other backends such as one or more ReLU layers instead of the hyperbolic tangent layer, but found no significant gains in validation losses. Before doing any other optimization, we found the optimal number l of LSTM nodes under the assumption that $l = 2^i$ for $i = 1, 2, \dots, 7$. The reason that we could use a rather small upper bound for the number of nodes is that we did not use datasets such as those from NLP that require a big memorization ability.

The next topic is hyperparameter optimization. Choi et. al. (Choi et al., 2019) found that comparisons of different weight optimizers such as ADAM (Kingma and Ba, 2014) and NADAM (Dozat, 2016) often is skewed by inadequate hyperparameter optimization and recommend that all parameters in the algorithms should be optimized. We used their methodology with the initial parameter ranges that they give in Appendix D.8 for every single dataset. As they recommend, we performed a random search within these ranges but used many more evaluations, namely 512 random parameter sets for each dataset and picked the best one for each dataset using the validation data. Thus, we optimized all parameters in the ADAM algorithm and not just the learning rate.

We tried with both ADAM and NADAM, but the difference between them was negligible. ADAM was used in all subsequent experiments.

We also used the same learning rate schedule as Choi et. al. (Choi et al., 2019), namely the one from Shallue et. al. (Shallue et al., 2019), and optimized the initial learning rate, the duration of the decay and the amount of decay together with the ADAM hyperparameters. Our batch size is so small that no warm-up is needed.

The amount of training is often measured in the number of epochs, but we will instead use the total number of training examples including duplicates, that is the number of epochs times the training set cardinality. Each training session consisted of running 320 000 training examples with a batch size of four, that is a total of 80 000 weight updates. After preliminary experiments, we abandoned L1 and L2 regularization and dropout but chose to employ model checkpointing as follows. For every 20 000 training examples, we ran the net with the current weights on the validation data and updated the best weights found if there was a validation improvement.

4.2 Experiment design and implementation

A key challenge with ADATE as for many other evolutionary algorithms is that very many evaluations may be required, where evaluation means to compute an evaluation value, sometimes called “fitness”, for a solution candidate, which here is an ARN.

ADATE first screens candidates using a quite limited and very quick evaluation. The candidates that pass the screening, typically less than 1%, then move on to a second stage evaluation that in most cases use at least 100 times more time per candidate. Finally, less than 1% of the ones who pass the second stage are then passed to a third and final stage. The first two stages use a smaller number of training steps and a smaller number of recurrent nodes as follows.

First stage. The goal for this stage was to have an overall evaluation time for a new neuron that is less than 100 ms. For some CPUs and datasets, we achieved 50 ms and for other combinations it is up to 200 ms. Of course, the evaluation results will be very bad in this stage, but still enough to filter away really bad programs. The number of nodes was always four and we used only 5000 training examples. Additionally, we restricted the training to run on only the five last timesteps in each time series.

Second stage. Here, we use 40 000 training examples, all timesteps and $l/4$ nodes. In comparison with the first stage, the run time is increased by a factor given by the following expression where n_t is the number of time steps.

$$8 \cdot (l/16)^2 \cdot n_t/5$$

For example, with $l = 64$ and 100 time steps, the increase is 2560 times.

Third stage. This stage uses the full 320 000 training examples and l nodes. Thus, its expected run time is $8 \cdot 4^2$, that is 128, times longer than the second stage.

For say $l = 64$ and 100 timesteps, the total speed amplification is about $2560 \cdot 128/3$, that is about 10^5 times, since the implementation actually tries to spend equally long run time on each stage.

Our compiler translates a functional program that represents a neuron into byte code, which then is run on-the-fly by a byte code interpreter implemented in C++. Since matrix operations require almost all the execution time, it does not matter that neuron evaluation is somewhat slower than optimized machine code.

All of the neural net is also implemented in C++ and uses the automatic differentiation library AADC that kindly was made available by Matlogica Ltd, who also provided absolutely outstanding support for how to use it in the most efficient way, especially for matrix operations. The resulting vectorized machine code, that is AVX256 or optionally AVX512, appears to run several times faster than Tensorflow, when the latter is restricted to a single CPU core. We evaluated the C interfaces of all the leading neural net packages but did not find anything that could compete with the speed, stability and ease of use that characterizes AADC.

To check the correctness of our implementation, we ran the same datasets with LSTM using both our C++ code and Tensorflow and compared the results. Additionally, we implemented one of the new neurons in Tensorflow and compared with the C++ code without finding any statistically significant differences. All comparisons and other experiments used 64-bit floating point numbers since a 32-bit AADC version was not yet available from Matlogica.

An ADATE run used between 500 and 1000 CPU cores depending on what was available. The number of evaluated candidate neurons was on the order of one billion for each dataset and around three days of run time were typically needed to find the best results.

4.3 Datasets

Since we need to evaluate new neurons rather quickly, we chose to focus on datasets that can be effectively run with 128 LSTM neurons or less, that is rather small nets. For this

reason, we avoided speech and NLP datasets that typically require bigger nets as well as attention (Bahdanau et al., 2014; Graves, 2013) to get the best results.

Many of the datasets come from the excellent online repository for time series datasets that is curated by Bagnall et. al. (Bagnall et al., 2017) and their time series classification (TSC) research group. Most of the datasets are time series from various physical sensors.

The only preprocessing that we employed was either centering and scaling or one hot encoding, depending on whether a predictor or an output was ordinal or nominal. Note that the goal of the experiments is a reliable comparison between LSTM and new neurons and not to get state-of-the-art results for any dataset. For this reason, we did not do any feature engineering or data augmentation. Thus, due to not doing any more advanced preprocessing, our results may for some datasets be far from the best that is possible.

We will first give a brief description of each dataset and then list the number of examples, that is time series, and the number of predictors for each one.

3W This is a predictive maintenance dataset that was donated to the UCI machine learning repository by Petrobras (Vargas et al., 2019) and consists of actual sensor values and events in oil wells supplemented by simulated and handcrafted values and events. The task is to predict undesirable events. We preprocessed the dataset into non-overlapping time windows and used only sensor readings, for example temperature and pressure, as predictors.

Crop This dataset is from TSC but was originally collected by Tan et. al. (Tan et al., 2017). The goal is to classify the type of crop on a patch of land from the time series of images produced by the Sentinel-2A satellite, which has plant growth monitoring as one of its primary missions.

Double pendulum The task of the RNN is to learn to simulate a double pendulum. In general, RNNs can be applied to modeling of chemical and physical processes and are, for example, used quite successfully for this purpose by the Borregaard biorefinery since the beginning of 2022. Inspired by this, we generated the Double Pendulum dataset from the simulation provided with the SimBody physics engine. The predictors are the center of gravity coordinates of the first as well as the second pendulum at a given timestep and the response is the corresponding coordinates for the next timestep. Each time series is generated from randomly chosen initial positions and angular velocities. We deliberately lowered the sampling frequency so that black box modeling from measurement data alone becomes challenging.

ECG5000 This dataset is a 20-hour long ECG and was originally published by Goldberger et. al. (Goldberger et al., 2000), who preprocessed the signals to make each heartbeat equally long using interpolation. We downloaded it from TSC.

FordB This dataset was originally used in a competition at WCCI 2008 (Abou-Nasr and Feldkamp, 2008) and the task is to determine if there is something wrong with an internal combustion engine based on recordings of the engine sound. This dataset was also taken from TSC.

Insect wingbeat This dataset (Chen et al., 2014) contains spectrograms from the sounds generated by the wings of insects, in this case mostly mosquitoes and flies. The goal

Table 1: Number of examples, number of timesteps, number of inputs and number of outputs after one hot encoding.

Dataset	#examples	#timesteps	#inputs	#outputs
3W	2864	64	8	17
Crop	24000	46	1	24
Double pendulum	10000	128	4	4
ECG5000	5000	140	1	5
FordB	3836	500	1	2
Insect wingbeat	20000	22	200	10
LSST	4925	36	6	14
WISDM	27540	40	3	6

is to classify the species of an insect based on a sound recording. We downloaded it from TSC.

LSST This is yet another TSC dataset but originally comes from a 2018 Kaggle competition (Allam Jr et al., 2018). It contains simulated data from the Vera C. Rubin Observatory, also known as the Large Synoptic Survey Telescope (LSST), that are measurements of how the brightness of an astronomical object varies with time. The goal is to determine which kind of object that was observed.

WISDM The task is to predict the activity of a cell phone user based on the time series of accelerometer values (Kwapisz et al., 2011). We used the most difficult version of the WISDM dataset which is version 1.1 without overlapping time windows and downloaded it from the UCI machine learning repository.

As can be seen in Table 1, most of the datasets have a small or medium number of examples. This is a use case which is just as important as big data since many datasets that arise in practice have sizes similar to those in the table. Indeed, most datasets gathered by TSC are even smaller, but we did not want to include these since the confidence intervals may become too big.

4.4 Experimental results

Table 2 compares an LSTM net with an ARN net for the test data sets. We used categorical cross entropy (CCE) for the classification datasets and mean squared error (MSE) for the regression dataset. The p-value was calculated using McNemar’s test for classification and the Wilcoxon signed-rank test for regression with continuity correction in both cases. As can be seen in Table 2, the p-values are better than five sigma for six of the eight datasets.

The column “Factor better” shows how many times better the ARN was compared with LSTM with respect to CCE or MSE.

Since we carefully optimized the hyperparameters for LSTM, the big improvements obtained for say 3W, Double pendulum, Ford B, LSST and WISDM, cannot be explained by the LSTMs being poorly tuned. Instead, the most likely explanation is that the new ARN neurons have a superior modeling and fitting ability.

Table 2: Test data cross entropies or MSE and accuracies for LSTM and ARN.

Dataset	LSTM CCE/MSE	ARN CCE/MSE	Factor better	LSTM Acc	ARN Acc	p-value
3W	0.517	0.303	1.71	0.804	0.934	$1.2 \cdot 10^{-18}$
Crop	0.796	0.661	1.20	0.742	0.775	$3.8 \cdot 10^{-11}$
Pendulum	0.154	0.110	1.40			$1.1 \cdot 10^{-19}$
ECG5000	0.188	0.188	1	0.949	0.947	0.74
FordB	0.510	0.140	3.64	0.759	0.950	$3.6 \cdot 10^{-31}$
Wingbeat	1.120	1.029	1.09	0.574	0.605	$1.0 \cdot 10^{-5}$
LSST	1.598	1.183	1.35	0.478	0.627	$1.1 \cdot 10^{-21}$
WISDM	0.137	0.081	1.69	0.963	0.975	$3.5 \cdot 10^{-8}$

As can be seen in the table, the improvement that was obtained varies a lot between the datasets. For example, for the FordB dataset, we obtained a more than three-fold reduction of the test data CCE, whereas there was no improvement at all for the ECG5000 dataset. One possible explanation for the huge improvement for FordB is that this dataset has as many as 500 timesteps and that LSTM cannot effectively handle so long time dependencies, whereas ARN can do that using skip connections through time. By looking at the best program for FordB in Appendix A.4, it is easy to see that skip connections are indeed used, but otherwise this is a really hard neuron to analyze since it was not designed by human beings.

Since the experiments optimized cross entropy instead of accuracy, it is likely that somewhat higher accuracies could be obtained if ADATE were to directly optimize the accuracy instead.

We omitted the neuron for ECG5000 since it was no improvement, but the best ones for all the other datasets are listed in the appendices. As can be seen there, there is a huge variation from one dataset to the next, but both skip connections and the linear combinations of state 0 (`OtherPeepsLC`) are frequently used. From the outset, we naively guessed that reading the memories of other neurons would give rise to problems akin to vanishing or exploding gradients, but this seems to be much less problematic than we thought.

All of the best programs use novel activation functions that we have never seen before. For example, the best program for WISDM in Appendix A.7 uses `srelu` applied to quadratic forms in several places. Many of the other neurons also contain various quadratic expressions, but which roles they have is not clear.

There are some obvious redundancies in the coding, for example applying `relu` twice. ADATE is able to remove such redundancies, but much more run time might be needed.

In general, evolution in ADATE is so effective that neurons are likely to become exquisitely adapted to the special characteristics of the dataset. This means that neurons should not be reused from one class of datasets to the next, that is, a new ADATE run is needed for each new type of application. One way to avoid this special adaption would be to run on say hundreds of different datasets simultaneously using many more cores and possibly accelerators.

4.5 A closer look at some ARNs

In this section, we will discuss the circuit diagrams for the best LSST neuron and the best FordB neuron. These were selected since they are among the simpler best neurons. In order to translate the neuron syntax from SML to diagrams, we first printed them as C expressions using our compiler, converted them to equations and then manually simplified these equations before using them to draw the neurons.

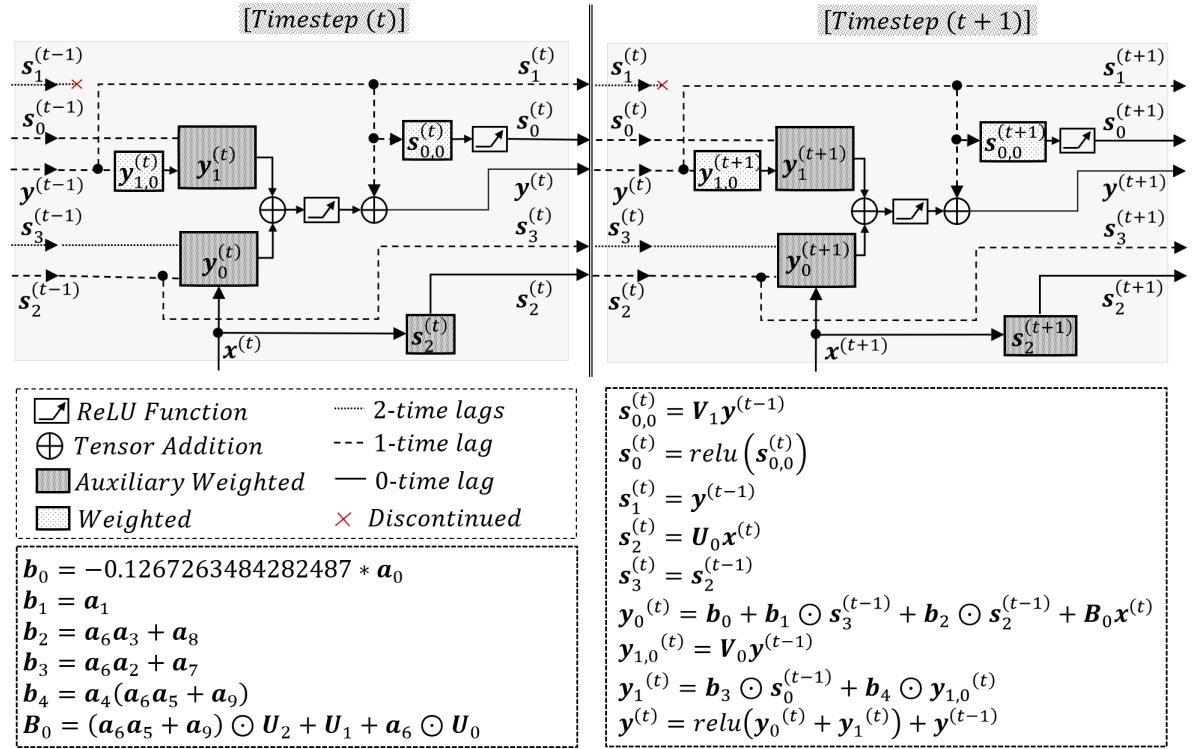


Figure 4: A circuit diagram for the best neuron for the LSST dataset .

Both the diagram and the equations for LSST are shown in Figure 4. All vector-vector multiplications are element-wise and all variables denoted by \mathbf{b} or \mathbf{B} are vectors or matrices manually derived from `cons` expressions in the SML code that after translation to C contains auxiliary weights, denoted by \mathbf{a} variables. We do not show the full and lengthy manual translation from SML to simplified equations.

It is a bit fascinating to see that ADATE actually has invented a small convolutional filter represented by the equation for $y_0^{(t)}$. This filter combines the inputs from three consecutive timesteps using a linear combination. However, the output from the filter is combined with skip connections from previous outputs represented by $y_1^{(t)}$. Thus, the convolution is in principle over inputs and some outputs and the result is fed to `relu` as can be seen in the equation for $y^{(t)}$.

Another interesting feature of this neuron is that it totally has abandoned **tanh** and **srelu** as activation functions. As can be seen in Figure 4, it only contains two **relu** functions. However, we are not able to theoretically understand the dynamic behaviour of RNNs that contain such neurons and can only claim that it produces superior accuracy for the LSST dataset.

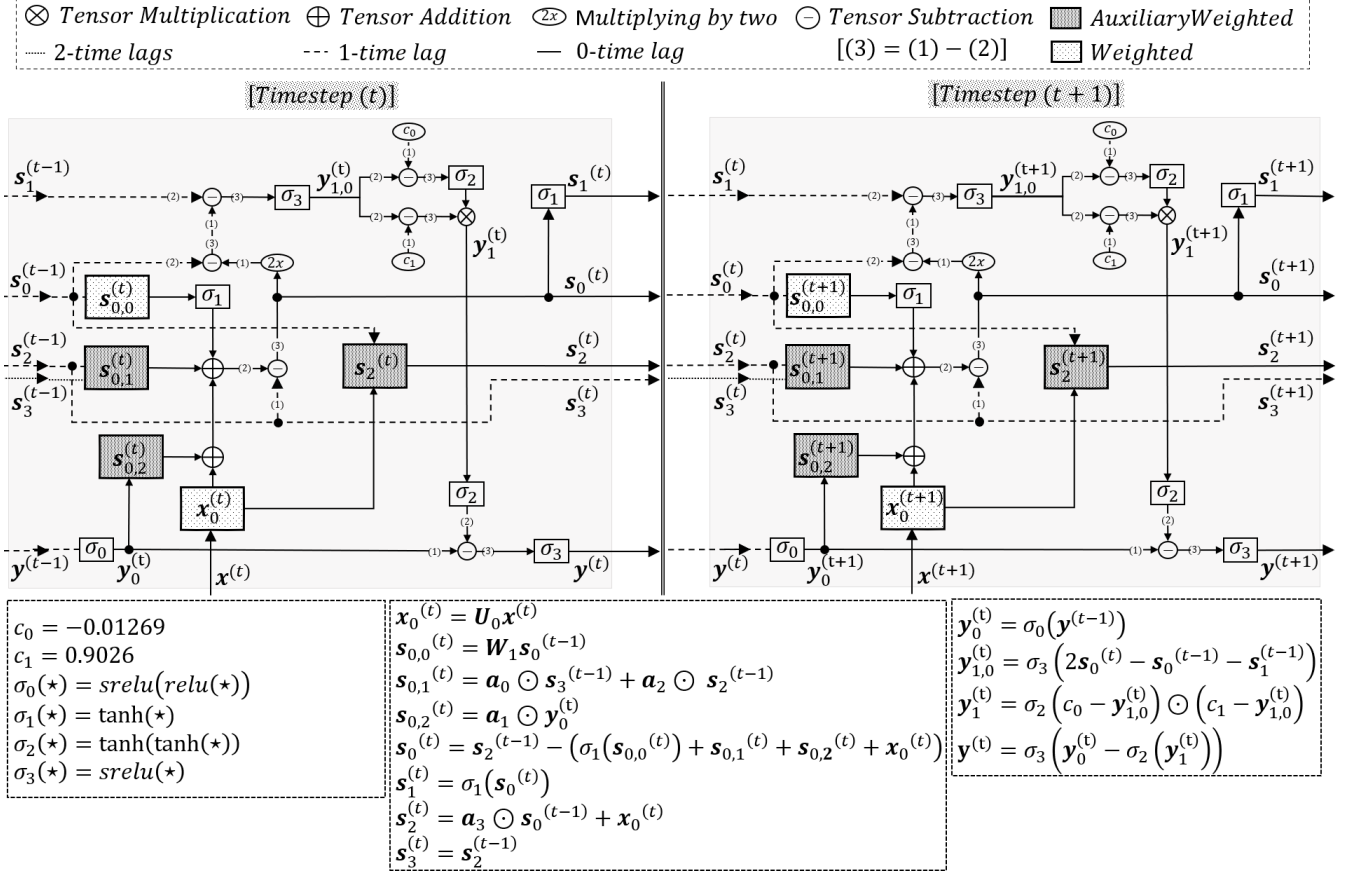


Figure 5: A circuit diagram for the best neuron for the FordB dataset .

The best neuron for the FordB dataset is more complex and shown in Figure 5. We will now take a look at some elaborate skip connections in this neuron that use the output from time $t - 4$ to calculate the output at time t . Since the dataset contains 500 timesteps, we can speculate that it is especially important to curate information over long time periods and that special connections may have been evolved to handle that.

Let \rightarrow mean that the left hand side is partially used to compute the right hand side. Then, the information flow from $y^{(t-4)}$ to $y^{(t)}$ is as follows as can be seen in the circuit diagram.

$$y^{(t-4)} \rightarrow s_0^{(t-3)} \rightarrow s_2^{(t-2)} \rightarrow s_3^{(t-1)} \rightarrow y^{(t)}$$

Thus, the internal states are employed to implement information flow that appears to be custom designed to retain long term memory for the FordB dataset.

As a curiosity, we can just mention that ADATE has discovered ARNs that retain long term memory much better than LSTM for thousands of timesteps when simulating complex Mealy machines.

4.6 Analysis of a Pareto front

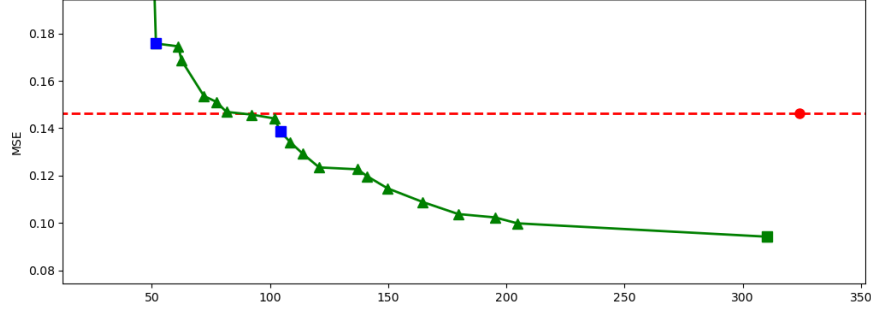


Figure 6: The Pareto front for Double pendulum.

Recall that a Pareto front contains gradually bigger and better programs so that the smallest and worst program comes first whereas the last program is the biggest and the best. As an example, we will use the Pareto front for the Double pendulum dataset which consists of 24 programs. The first four of these are so small that they are not interesting but the last 20 are shown in Figure 6. For this dataset, an LSTM has a validation MSE of 0.146 as indicated by the horizontal line in Figure 6, which means that all programs below the line are better than LSTM for Double pendulum on validation data.

By using Pareto fronts, ADATE tries to both minimize MSE and program size. This has been so successful that all programs in the front are smaller, at least according to the ADATE syntactic complexity, than the LSTM program, which has a size of 324 bits. Thus, ADATE has found a plethora of programs that are both smaller and better than LSTM for Double pendulum.

We will take a closer look at the two programs that are indicated by the blue squares in Figure 6. The smallest one, corresponding to the leftmost square, has an MSE of 0.176 and is the following simple RNN, where no internal neuron states are used. Therefore, we have also manually edited the program to remove them

```
relu( lc2( cons( lc1( OtherOutputsLC ), InputsLC ) ) )
```

This is easy to understand and just a linear combination of the inputs and the outputs from other neurons, albeit formulated as a linear combination of a linear combination. Apparently, `relu` is more suitable than the other activation functions.

The next square square in Figure 6 is the program in Figure 2 that has an MSE of 0.139, which is better than for the LSTM.

Even if this neuron is quite simple, it is already becoming hard to understand exactly why it is better, with analysis being impeded by the use of internal states from other neurons. A partial hypothesis may be that using quadratic base functions may give more suitable regression modeling of a double pendulum.

The best neuron for Double Pendulum, which is the green and last square in Figure 6, is given in Appendix A.3. It is much better and has an MSE of 0.094 on validation data. It is also much more difficult to understand.

Also, note that the test data MSE for this neuron is 0.11 and that using validation data for both hyperparameter optimization, ADATE runs, and model checkpointing leads to some overfitting on validation data. In spite of this, the neuron is significantly better than LSTM also on test data with a p-value around 10^{-19} .

The syntactic complexity makes a big jump with little gain in MSE from the second last to the best program in the front. Due to Ockhams’s razor (of Ockham, 1323), overfitting can be suspected when this happens.

5. Conclusions and future work

We tested the ADATE recurrent neurons (ARNs) on eight datasets. For the four best datasets, the ARNs were a factor of 3.6, 1.7, 1.7 and 1.4 better respectively as measured by cross entropy or mean squared error on test data. The p-values for these four were below about 10^{-18} , which is clearly better than five sigma.

For the other four datasets, there were significant improvements for three but failure for one. The reason it did not work for one dataset seems to be overfitting to the validation data caused by a combination of hyperparameter tuning, model check pointing and using validation data to calculate evaluation values for programs generated by ADATE and selecting the best one.

The results are so good that ARNs should be tried in practice whenever recurrent nets are used. The reasons for the big improvements that were found for at least half of the datasets are as follows.

1. ADATE is quite capable when it comes to automatically adapting the code of a neuron to a specific class of datasets.
2. The ARNs contain several somewhat unusual ingredients such as
 - (a) Up to four internal states per neuron. Sometimes, these are apparently used by ADATE to construct intricate skip connections through time.
 - (b) Linear combinations of the states of other neurons in addition to the usual combinations of outputs.
 - (c) Custom made activation functions that sometimes contain quadratic forms.
 - (d) Differentiation between “self” and “all others”.

The technology is ready to use right away in C++ with an option to manually port to Tensorflow. We encourage people interested in using it to contact the corresponding author of this paper. However, a cluster with between 500 and 1000 cores is needed to

run on a subset of data with up to about 50 000 training examples for about three days. Thus, the number of datasets that can be processed may be somewhat limited by available computational resources.

Here are some possibilities for future work.

1. Let an ARN layer be an ensemble of different neuron types and use ADATE to evolve all the different types, either one type at a time or all types simultaneously.
2. Use many stacked ARN layers with different neuron types in each layer.
3. Find a way to efficiently optimize hyperparameters as a part of the evolution instead of doing it only once at the beginning.
4. Run on hundreds of datasets during the same evaluation in order to find neurons that are generally better. However, we expect that evolving neurons for specific classes of datasets often will yield much better results.
5. Study other neural architectures than RNNs. For example, the batch normalization and ResNet blocks in a CNN could be viewed as the function \mathbf{f} to improve and the time dimension in an RNN could be replaced by a layer index dimension, where say four states per block are curated from one layer to the next by \mathbf{f} .
6. Another possibility would be define differentiable functional programs and neural nets that represent them. These could use differentiable datastructures and handle recursion using a predefined set of differentiable schemas that are generalizations of say catamorphisms, anamorphisms and hylo-morphisms.

It may also be possible to employ the automatic programming presented in this paper for a variety of other current and future neural net and differentiable programming technologies.

Appendix A. The best neurons according to validation data

This appendix lists the best programs according to validation data for the seven datasets out of eight for which improvements were found. They are presented exactly as they were printed by the ADATE system and could typically be somewhat simplified manually. Thus, they may look more complex than they really are.

The best neuron for WISDM has also been implemented by one of us as a custom layer in Tensorflow in addition to the automatically generated C++ code that our compiler generates based on the SML programs.

Requests for neuron synthesis and C++ or Tensorflow implementations for other datasets are very welcome.

Appendix A.1. The best ARN for 3W

```
fun f
  (
    SelfPeep0,
    SelfPeep1,
```

```

    SelfPeep2,
    SelfPeep3,
    SelfOutput,
    OtherPeepsLC,
    OtherOutputsLC,
    InputsLC
  ) =
case cons( SelfOutput, cons( SelfOutput, InputsLC ) ) of
  V21902689 =>
case
  (
    SelfOutput,
    tanh(
      srelu(
        (
          (
            lc3( cons( lc1( V21902689 ), V21902689 ) ) *
            srelu( SelfPeep3 )
          ) -
          (
            tanh(
              lc0(
                cons(
                  SelfPeep3,
                  cons( tanh( SelfOutput ), InputsLC )
                )
              ) +
              srelu(
                relu(
                  tanh(
                    lc2(
                      cons(
                        ~0.14531347527330391E~1,
                        cons(
                          SelfPeep3,
                          cons(
                            srelu( srelu( SelfPeep2 ) ),
                            cons(
                              SelfOutput,
                              cons( SelfPeep0, InputsLC )
                            )
                          )
                        )
                      )
                    )
                  )
                )
              )
            )
          )
        )
      )
    )
  )

```

```

    )
  )
) of
( V21915A57, V21915A58 ) =>
(
  V21915A58,
  SelfPeep0,
  srelu( relu( lc2( OtherOutputsLC ) ) ),
  SelfPeep0,
  srelu(
    (
      V21915A57 -
      relu(
        tanh(
          tanh(
            srelu(
              srelu(
                case ( SelfPeep1, V21915A58 ) of
                  ( V21915A59, V21915A5A ) =>
                    ( V21915A5A - V21915A59 )
                )
              )
            )
          )
        )
      )
    )
  )
)

```

Appendix A.2. The best ARN for Crop

```
fun f
  (
    SelfPeep0,
    SelfPeep1,
    SelfPeep2,
    SelfPeep3,
    SelfOutput,
    OtherPeepsLC,
```

```

    OtherOutputsLC,
    InputsLC
  ) =
case
  (
    SelfOutput,
    (
      ( lc3( OtherPeepsLC ) * lc0( InputsLC ) ) -
      (
        tanh(
          srelu(
            lc0(
              cons(
                SelfPeep1,
                cons(
                  SelfPeep3,
                  cons( lc4( OtherPeepsLC ), bias )
                )
              )
            )
          ) +
          lc3( InputsLC )
        )
      ) of
      ( VDBC64A, VDBC64B ) =>
case srelu( srelu( ( VDBC64B - SelfPeep1 ) ) ) of
  V1C427005 =>
    (
      VDBC64B,
      SelfPeep0,
      lc0( cons( SelfPeep0, OtherPeepsLC ) ),
      SelfPeep2,
      srelu(
        case ( V1C427005, V1C427005 ) of
          ( V1C481BD5, V1C481BD6 ) =>
            let
              fun g1CDF7C46 V1CDF7C47 =
                ( VDBC64A - V1CDF7C47 )
            in
              g1CDF7C46( ( V1C481BD6 * V1C481BD5 ) )
            end
          )
        )
    )
  )

```

Appendix A.3. The best ARN for Double pendulum

```

fun f
  (
    SelfPeep0,
    SelfPeep1,
    SelfPeep2,
    SelfPeep3,
    SelfOutput,
    OtherPeepsLC,
    OtherOutputsLC,
    InputsLC
  ) =
  (
    (
      (
        relu( relu( lc1( cons( lc1( OtherPeepsLC ), InputsLC ) ) ) ) -
        relu(
          lc3(
            cons(
              lc4( OtherPeepsLC ),
              cons( 0.22174599383632232, InputsLC )
            )
          )
        ),
        SelfPeep1,
        SelfPeep2,
        SelfPeep3,
        (
          (
            (
              lc4(
                cons(
                  lc4( OtherPeepsLC ),
                  cons(
                    lc0(
                      cons(
                        SelfPeep2,
                        cons(
                          ( ~0.6961519103176064 + SelfPeep1 ),
                          InputsLC
                        )
                      )
                    )
                  )
                ),
                InputsLC
              )
            ),
            SelfOutput
          )
        )
      )
    )
  )

```

```

    )
  )
) *
lc0( OtherPeepsLC )
) +
SelfPeep0
) *
(
SelfPeep1 -
(
  tanh(
    case
      cons(
        lc3(
          cons(
            SelfPeep2,
            cons( ~0.6961519103176064, InputsLC )
          )
        ),
        InputsLC
      ) of
V1662138D =>
(
  srelu(
    lc0(
      cons(
        SelfPeep0,
        cons( lc0( V1662138D ), InputsLC )
      )
    )
  ) *
  srelu(
    lc0(
      cons(
        relu(
          lc3(
            cons(
              SelfPeep0,
              cons(
                lc0(
                  cons( lc0( V1662138D ), V1662138D )
                ),
                InputsLC
              )
            )
          )
        )
      )
    )
  )
)

```



```

    )
  ),
  InputsLC
)
)
)
)
) +
~0.45284110969509517
)
)
)
)
)

```

Appendix A.4. The best ARN for FordB

```

fun f
(
  SelfPeep0,
  SelfPeep1,
  SelfPeep2,
  SelfPeep3,
  SelfOutput,
  OtherPeepsLC,
  OtherOutputsLC,
  InputsLC
) =
case srelu( srelu( relu( relu( SelfOutput ) ) ) ) of
  V281AF3E7 =>
case
(
  V281AF3E7,
  (
    SelfPeep2 -
    (
      tanh( lc1( OtherPeepsLC ) ) +
      lc0(
        cons(
          SelfPeep3,
          cons( V281AF3E7, cons( SelfPeep2, InputsLC ) )
        )
      )
    )
  )
) of

```

```

( VDBC64A, VDBC64B ) =>
(
  VDBC64B,
  tanh( srelu( srelu( VDBC64B ) ) ),
  lc0( cons( tanh( SelfPeep0 ), InputsLC ) ),
  SelfPeep2,
  srelu(
    (
      VDBC64A -
    (
      case
      case
      let
      fun g1C57E5DF V1C57E5E0 =
      (
        V1C57E5E0,
        (
          ~0.12690104588539253E~1 -
        (
          case ( VDBC64B, SelfPeep1 ) of
            ( V1C57EDC3, V1C57EDC4 ) =>
              srelu(
                (
                  ( V1C57EDC3 - SelfPeep0 ) +
                  ( V1C57EDC3 - V1C57EDC4 )
                )
              ) )
        )
      )
    )
  )
  in
    g1C57E5DF(
      case g1C57E5DF 0.1029527350644156 of
        ( A, B ) => A + B
      )
    end
    of
      ( V5FAAD0B, V5FAAD0C ) =>
        ( V5FAAD0B, srelu( V5FAAD0C ) )
      of
        ( V1D190879, V1D19087A ) =>
          tanh( tanh( ( V1D19087A * V1D190879 ) ) ) )
    )
  )
)

```

Appendix A.5. The best ARN for Insect wingbeat

```

fun f
(

```

```

SelfPeep0,
SelfPeep1,
SelfPeep2,
SelfPeep3,
SelfOutput,
OtherPeepsLC,
OtherOutputsLC,
InputsLC
) =
case
(
SelfOutput,
(
(
srelu(
tanh(
tanh(
lc3(
cons(
0.10022791851659179E1,
cons( lc4( OtherOutputsLC ), InputsLC )
)
)
)
) *
srelu( tanh( lc0( InputsLC ) ) )
) -
(
tanh( srelu( ~0.6873893912995532E~2 ) ) +
srelu( relu( SelfOutput ) )
)
)
) of
( VDBC64A, VDBC64B ) =>
case tanh( srelu( srelu( tanh( relu( VDBC64B ) ) ) ) ) of
V1C9C2AC6 =>
case ( V1C9C2AC6, V1C9C2AC6 ) of
( V1C9C2AD2, V1C9C2AD3 ) =>
(
VDBC64B,
( tanh( SelfPeep2 ) * SelfPeep3 ),
relu( tanh( relu( V1C9C2AD3 ) ) ),
SelfPeep2,
srelu( ( VDBC64A - tanh( V1C9C2AD2 ) ) )

```

)

Appendix A.6. The best ARN for LSST

```

fun f
  (
    SelfPeep0,
    SelfPeep1,
    SelfPeep2,
    SelfPeep3,
    SelfOutput,
    OtherPeepsLC,
    OtherOutputsLC,
    InputsLC
  ) =
  (
    relu( lc1( OtherOutputsLC ) ),
    SelfOutput,
    lc0( InputsLC ),
    SelfPeep2,
    (
      relu(
        lc1(
          cons(
            srelu( ~0.1267263484282487 ),
            cons(
              SelfPeep3,
              case
                cons(
                  SelfPeep0,
                  cons(
                    SelfPeep2,
                    cons(
                      lc2( cons( lc0( OtherOutputsLC ), InputsLC ) ),
                      InputsLC
                    )
                  )
                )
              of
                V259F26F2 => cons( lc0( V259F26F2 ), V259F26F2 )
            )
          )
        )
      ) +
    SelfOutput
  )

```

)

Appendix A.7. The best ARN for WISDM

```

fun f
  (
    SelfPeep0,
    SelfPeep1,
    SelfPeep2,
    SelfPeep3,
    SelfOutput,
    OtherPeepsLC,
    OtherOutputsLC,
    InputsLC
  ) =
case
  (
    SelfOutput,
    (
      lc0( bias ) -
      (
        tanh(
          srelu(
            srelu(
              lc1(
                cons(
                  SelfPeep1,
                  cons(
                    SelfPeep3,
                    cons(
                      (
                        lc4( InputsLC ) *
                        lc2( cons( SelfPeep0, InputsLC ) )
                      ),
                      cons(
                        srelu(
                          relu(
                            lc2(
                              cons(
                                lc0( OtherOutputsLC ),
                                OtherPeepsLC
                              )
                            )
                          )
                        )
                      )
                    )
                  ),
                ),
              ),
            ),
          ),
        ),
      ),
    ),
  ),

```

```

        case
        cons( lc1( OtherPeepsLC ), InputsLC )
      of
        V271482D0 =>
          cons( lc2( V271482D0 ), V271482D0 )
        )
      )
    )
  )
) +
srelu(
  relu( lc2( cons( lc4( OtherPeepsLC ), InputsLC ) ) )
)
)
) of
( VDBC64A, VDBC64B ) =>
(
  VDBC64B,
  SelfPeep0,
  srelu( srelu( srelu( lc0( OtherPeepsLC ) ) ) ),
  SelfPeep2,
  srelu(
    (
      VDBC64A -
      (
        ( VDBC64B - SelfPeep1 ) *
        ( VDBC64B - SelfPeep1 )
      )
    )
  )
)
)

```

References

- M. Abou-Nasr and L. Feldkamp. Ford classification challenge. *Competition organized in conjunction with the IEEE World Congress on Computational Intelligence (WCCI 2008)*, 2008.
- T. Allam Jr, A. Bahmanyar, R. Biswas, M. Dai, L. Galbany, R. Hložek, E. E. Ishida, S. W. Jha, D. O. Jones, R. Kessler, et al. The photometric lsst astronomical time-series classification challenge (plasticc): Data set. *arXiv preprint arXiv:1810.00001*, 2018.

- A. Bagnall, J. Lines, A. Bostrom, J. Large, and E. Keogh. The great time series classification bake off: a review and experimental evaluation of recent algorithmic advances. *Data Mining and Knowledge Discovery*, 31:606–660, 2017.
- D. Bahdanau, K. Cho, and Y. Bengio. Neural machine translation by jointly learning to align and translate. *arXiv preprint arXiv:1409.0473*, 2014.
- J. Bayer, D. Wierstra, J. Togelius, and J. Schmidhuber. Evolving memory cell structures for sequence learning. In *International conference on artificial neural networks*, pages 755–764. Springer, 2009.
- H. Berg, R. Olsson, T. Lindblad, and J. Chilo. Automatic design of pulse coupled neurons for image segmentation. *Neurocomputing*, 71(10-12):1980–1993, 2008.
- Y. Chen, A. Why, G. Batista, A. Mafra-Neto, and E. Keogh. Flying insect classification with inexpensive sensors. *Journal of insect behavior*, 27(5):657–677, 2014.
- K. Cho, B. Van Merriënboer, D. Bahdanau, and Y. Bengio. On the properties of neural machine translation: Encoder-decoder approaches. *arXiv preprint arXiv:1409.1259*, 2014.
- D. Choi, C. J. Shallue, Z. Nado, J. Lee, C. J. Maddison, and G. E. Dahl. On empirical comparisons of optimizers for deep learning. *arXiv preprint arXiv:1910.05446*, 2019.
- T. Dozat. Incorporating nesterov momentum into adam. *Project report for CS229, Stanford University*, 2016.
- K. Fukushima. Visual feature extraction by a multilayered network of analog threshold elements. *IEEE Transactions on Systems Science and Cybernetics*, 5(4):322–333, 1969.
- E. Galván and P. Mooney. Neuroevolution in deep neural networks: Current trends and future challenges. *IEEE Transactions on Artificial Intelligence*, 2(6):476–493, 2021.
- A. L. Goldberger, L. A. Amaral, L. Glass, J. M. Hausdorff, P. C. Ivanov, R. G. Mark, J. E. Mietus, G. B. Moody, C.-K. Peng, and H. E. Stanley. Physiobank, physiokit, and physionet: components of a new research resource for complex physiologic signals. *Circulation*, 101(23):215–220, 2000.
- M. Gordon, R. Milner, L. Morris, M. Newey, and C. Wadsworth. A metalanguage for interactive proof in lcf. In *Proceedings of the 5th ACM SIGACT-SIGPLAN symposium on Principles of programming languages*, pages 119–130, 1978.
- A. Graves. Generating sequences with recurrent neural networks. *arXiv preprint arXiv:1308.0850*, 2013.
- K. Greff, R. K. Srivastava, J. Koutník, B. R. Steunebrink, and J. Schmidhuber. Lstm: A search space odyssey. *IEEE transactions on neural networks and learning systems*, 28(10):2222–2232, 2016.
- S. Hochreiter and J. Schmidhuber. Long short-term memory. *Neural computation*, 9(8):1735–1780, 1997.

- R. Jozefowicz, W. Zaremba, and I. Sutskever. An empirical exploration of recurrent network architectures. In *International conference on machine learning*, pages 2342–2350. PMLR, 2015.
- D. P. Kingma and J. Ba. Adam: A method for stochastic optimization. *arXiv preprint arXiv:1412.6980*, 2014.
- E. Kitzelmann, U. Schmid, R. Olsson, and L. P. Kaelbling. Inductive synthesis of functional programs: An explanation based generalization approach. *Journal of Machine Learning Research*, 7(2), 2006.
- J. R. Kwapisz, G. M. Weiss, and S. A. Moore. Activity recognition using cell phone accelerometers. *ACM SigKDD Explorations Newsletter*, 12(2):74–82, 2011.
- S. Li, W. Li, C. Cook, C. Zhu, and Y. Gao. Independently recurrent neural network (indrnn): Building a longer and deeper rnn. In *Proceedings of the IEEE conference on computer vision and pattern recognition*, pages 5457–5466, 2018.
- R. Milner, M. Tofte, R. Harper, and D. MacQueen. *The definition of standard ML: revised*. MIT press, 1997.
- W. of Ockham. *Summa Totius Logicae*. University of Oxford, 1323.
- R. Olsson. Inductive functional programming using incremental program transformation. *Artificial intelligence*, 74(1):55–81, 1995.
- C. J. Shallue, J. Lee, J. Antognini, J. Sohl-Dickstein, R. Frostig, and G. E. Dahl. Measuring the effects of data parallelism on neural network training. *Journal of Machine Learning Research*, 20(112):1–49, 2019.
- C. W. Tan, G. I. Webb, and F. Petitjean. Indexing and classifying gigabytes of time series under time warping. In *Proceedings of the 2017 SIAM international conference on data mining*, pages 282–290. SIAM, 2017.
- R. E. V. Vargas, C. J. Munaro, P. M. Ciarelli, A. G. Medeiros, B. G. do Amaral, D. C. Barrionuevo, J. C. D. de Araújo, J. L. Ribeiro, and L. P. Magalhaes. A realistic and public dataset with rare undesirable real events in oil wells. *Journal of Petroleum Science and Engineering*, 181:106223, 2019.